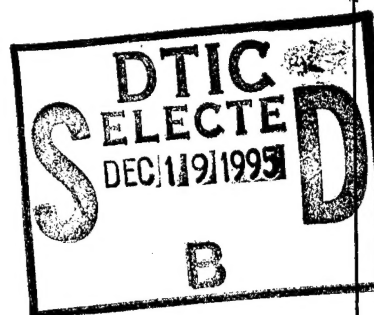


# U. S. Army Communications- Electronics Command

## Night Vision & Electronic Sensors Directorate

**Title:** Compact Mid-Infrared Source



**Author(s):** Dr. Walter R. Bosenberg

**Address:** Lightwave Electronics Corporation  
1161 San Antonio Road  
Mountain View, CA 94043

**Type of Report (Final, Interim, etc.):** Final

**Date:**

19951218 076

### Contract Number

DAAB07-95-C-M046

### Report Number

NV-96-C01

Approved for public release;  
distribution is unlimited.



Fort Belvoir, Virginia 22060-5806

## REPORT DOCUMENTATION PAGE

Form Approved  
OMB No. 0704-0188

1a. REPORT SECURITY CLASSIFICATION Unclassified		1b. RESTRICTIVE MARKINGS													
2a. SECURITY CLASSIFICATION AUTHORITY		3. DISTRIBUTION/AVAILABILITY OF REPORT Approved for Public Release; Distribution Unlimited													
2b. DECLASSIFICATION/DOWNGRADING SCHEDULE															
4. PERFORMING ORGANIZATION REPORT NUMBER(S)		5. MONITORING ORGANIZATION REPORT NUMBER(S) NV-96-C-01													
6a. NAME OF PERFORMING ORGANIZATION Lightwave Electronics Corp.	6b. OFFICE SYMBOL (If applicable)	7a. NAME OF MONITORING ORGANIZATION CECOM, Night Vision & Electronic Sensors Directorate													
6c. ADDRESS (City, State, and ZIP Code) 1161 San Antonio Rd Mountain View, CA 94043		7b. ADDRESS (City, State, and ZIP Code) NVESD 10221 Burbeck Rd STE 430 ATTN: AMSEL RD NV ST AL Fort Belvoir, VA 22060-5806													
8a. NAME OF FUNDING/SPONSORING ORGANIZATION	8b. OFFICE SYMBOL (If applicable)	9. PROCUREMENT INSTRUMENT IDENTIFICATION NUMBER DAAB07-95-C-M046													
8c. ADDRESS (City, State, and ZIP Code)		10. SOURCE OF FUNDING NUMBERS <table border="1"> <tr> <td>PROGRAM ELEMENT NO. 665502</td> <td>PROJECT NO. MM40</td> <td>TASK NO.</td> <td>WORK UNIT ACCESSION NO.</td> </tr> </table>		PROGRAM ELEMENT NO. 665502	PROJECT NO. MM40	TASK NO.	WORK UNIT ACCESSION NO.								
PROGRAM ELEMENT NO. 665502	PROJECT NO. MM40	TASK NO.	WORK UNIT ACCESSION NO.												
11. TITLE (Include Security Classification)  Compact Mid-Infrared Source															
12. PERSONAL AUTHOR(S) Dr. Walter R. Bosenberg															
13a. TYPE OF REPORT Final	13b. TIME COVERED FROM 3/10/95 TO 9/20/95	14. DATE OF REPORT (Year, Month, Day) 95 Sep 20	15. PAGE COUNT												
16. SUPPLEMENTARY NOTATION															
17. COSATI CODES <table border="1"> <tr> <th>FIELD</th> <th>GROUP</th> <th>SUB-GROUP</th> </tr> <tr> <td></td> <td></td> <td></td> </tr> <tr> <td></td> <td></td> <td></td> </tr> <tr> <td></td> <td></td> <td></td> </tr> </table>		FIELD	GROUP	SUB-GROUP										18. SUBJECT TERMS (Continue on reverse if necessary and identify by block number) Optical Parametric Oscillator; Quasi-Phase Match Material; Periodically Poled Lithium Niobate:	
FIELD	GROUP	SUB-GROUP													
19. ABSTRACT (Continue on reverse if necessary and identify by block number)  In this Phase I SBIR effort, we successfully demonstrated a high-power periodically-poled lithium niobate (PPLN) optical parametric oscillator (OPO) operating in the mid-infrared region of the spectrum. Highlighted experimental results are: (1) generation of 600 mW of 3.5 um radiation (from 5.8 W pump); (2) generation of 2 W of 1.54 um radiation (5.8 W pump); (3) operation at repetition rates of 5 - 32 kHz; (4) tuning over 2.7 um - 4.8 um (idler) and 1.35 - 1.66 um (signal); and (5) expanding our PPLN fabrication capabilities by poling full 3" diameter wafers, and poling 0.75 mm and 1.0 mm thick crystals. This work clearly demonstrates that PPLN OPOs are capable of generating high repetition rate mid-infrared radiation at Watt power levels.															
20. DISTRIBUTION/AVAILABILITY OF ABSTRACT <input type="checkbox"/> UNCLASSIFIED/UNLIMITED <input checked="" type="checkbox"/> SAME AS RPT. <input type="checkbox"/> DTIC USERS		21. ABSTRACT SECURITY CLASSIFICATION Unclassified													
22a. NAME OF RESPONSIBLE INDIVIDUAL Richard Utano		22b. TELEPHONE (Include Area Code) 703-704-3252	22c. OFFICE SYMBOL AMSEL RD NV ST AL												

## **Objectives of the Phase I program**

The goal of this Phase I SBIR effort was to investigate a compact and efficient mid-infrared laser source that operates in the 2 - 5  $\mu\text{m}$  range, based on a Nd:YAG laser pumping an optical parametric oscillator (OPO). A key feature to this work is the use of a new nonlinear optical material, Periodically-Poled Lithium Niobate (PPLN), in the OPO. Compared to other nonlinear materials used in OPOs in the mid-IR spectral region such as KTP, KTA, AgGaSe<sub>2</sub>, and ZnGeP<sub>2</sub>, PPLN has the combination of higher gain, lower loss, and noncritical phasematching at wavelengths less than ~4.5  $\mu\text{m}$ . Since PPLN is a new material, it is also relatively untested, particularly in the regime of high average power. This program demonstrated the feasibility of PPLN OPOs operating at the multi-watt power level.

The two main technical objectives for this Phase I program were as follows.

- To produce 1 W of 3.5  $\mu\text{m}$  radiation at a 10 kHz repetition rate.
- To improve the PPLN crystal fabrication process, yielding crystals of greater size and thickness.

## **Summary of the Phase I Results**

In this Phase I effort, we successfully demonstrated high power operation of a PPLN OPO operating in the mid-infrared region of the spectrum. Highlighted experimental results are given below and will be discussed in detail later in this report.

- Produced ~600 mW of 3.5  $\mu\text{m}$  radiation from 5.8 W of pump.
- Produced ~2 W of 1.54  $\mu\text{m}$  output from 5.8 W of pump.
- Operated the OPO at repetition rates of 5 - 32 kHz.
- Tuned the OPO over 2.7  $\mu\text{m}$  - 4.8  $\mu\text{m}$  (idler) and 1.35 - 1.66  $\mu\text{m}$  (signal).
- Demonstrated device quality fabrication of PPLN crystals on a 3" wafer scale.
- Demonstrated feasibility of poling 0.75 mm and 1.0 mm thick LiNbO<sub>3</sub>, but no device quality crystals were fabricated.

Classification	
<input checked="" type="checkbox"/> <input type="checkbox"/> <input type="checkbox"/>	
By _____	
Distribution/ _____	
Availability Codes	
Dist	Avail and/or Special
A-1	

## **Table of Contents**

1.0	Background for Phase I Research .....	3
2.0	Phase I Results.....	4
2.1	Fabrication of PPLN Material.....	5
2.2	PPLN OPO Results .....	8
2.2.1	The Pump Laser.....	8
2.2.2	The OPO Results.....	10
2.3	Phase I Conclusions.....	16
3.0	Potential Commercial Applications .....	17
3.1	Eye-safe laser radar and range finders .....	17
3.2	Hydrocarbon Detectors .....	18
4.0	Recommendations for Phase II .....	18
5.0	Conclusions.....	22
6.0	References.....	22

## 1.0 Background for Phase I Research

High power mid-infrared laser sources have long been sought for a variety of commercial and military applications. The use of optical parametric oscillators (OPOs) to convert the wavelength of fixed frequency near-infrared lasers to the mid-IR has been an active area of research for many years. Despite the active research, and the introduction of numerous commercial visible and near infrared OPO sources, no suitable high-power mid-IR laser sources have been developed that meet the requirements of the applications. The main barrier to the development of mid-IR OPO sources is the lack of suitable nonlinear optical materials. Despite demonstrations of OPOs using other materials such as KTP, KTA, AgGaSe<sub>2</sub>, ZnGeP<sub>2</sub>, and bulk LiNbO<sub>3</sub>, none of these materials adequately meets all the requirements for high-power mid-IR OPOs. Each material falls short on at least one of the important material requirements. For example, KTP has too much loss at wavelengths  $>3.2\text{ }\mu\text{m}$ . KTA has better transmission than KTP, but has unfavorable phasematching for wavelengths longer than  $3.6\text{ }\mu\text{m}$  resulting in large walkoff angles. The phasematching of AgGaSe<sub>2</sub> requires that it must be pumped at  $2\text{ }\mu\text{m}$ , and it suffers from a combination of high loss at  $2\text{ }\mu\text{m}$  ( $\sim 0.02\text{ cm}^{-1}$ ), and poor thermal conductivity limiting its mid-IR output to less than 1 W. Additionally, the low optical damage threshold of AgGaSe<sub>2</sub> makes operation of OPOs based on it damage prone and less rugged. ZnGeP<sub>2</sub> must also be pumped at  $2\text{ }\mu\text{m}$  and suffers from very high loss at the pump wavelength ( $>0.3\text{ cm}^{-1}$ ), but its high thermal conductivity has allowed it to produce the highest average power mid-IR radiation to date. ZnGeP<sub>2</sub> however is at present unsuitable for commercial applications, since each crystal costs  $\sim \$30,000$  and has a 6 month lead time. Bulk LiNbO<sub>3</sub> has been used in mid-IR OPOs for over 20 years; however, its low damage threshold makes this material unsuitable for commercial OPOs.

Periodically-poled lithium niobate (PPLN) is a "new" nonlinear material that has favorable properties relative to other materials. This material uses quasi-phasematching (QPM) rather than birefringent phasematching to achieve efficient frequency conversion. The concept of QPM is described in the literature [1,2] and in our Phase I proposal. The two main advantages of QPM in lithium niobate include higher gain (through the use of a larger nonlinear coefficient), and the ability to noncritically phasematch any frequency conversion process within the transparency range of the bulk crystal. The first advantage is obvious. By increasing the gain of the crystal the oscillation threshold is reduced, which decreases the likelihood of damage. PPLN OPOs have been operated over 25 times above threshold without optical damage, while bulk LiNbO<sub>3</sub> OPOs can only be operated  $<3\text{-}4$  times threshold without damage. The merit of the second advantage is less obvious, but equally important for high repetition rate (or low-peak power) OPOs. The decrease of

parametric gain due to walkoff is well-known [3,4]. Unfortunately, for angle-tuned birefringent phasematching (all of the crystals mentioned above use this type of phasematching), walkoff is a fact of life. Walkoff has a particularly negative effect when the beam sizes are small such as for low peak power (high repetition rate) OPOs. The ability of PPLN to phasematch any wavelength within its transparency range with zero walkoff, allows operation of the OPO at much higher repetition rates (e.g. lower peak powers). In this report, we describe operation of an OPO at over 30 kHz. Additionally, the "noncritical" nature of noncritical phasematching, allows for a much more rugged device.

PPLN has properties that make it an excellent candidate for high-power mid-IR generation; however, because it is so new, it is also untested. The goal of this Phase I program was to determine the feasibility of PPLN OPOs for generating high average power mid-IR radiation.

## 2.0 Phase I Results

The work plan of the proposal was altered in two places to reflect the difference in the state of the art that had occurred between the writing of the proposal and the start of program (~8 months). First, the proposal called for adapting an existing Lightwave laser to produce the shortest possible pulses at repetition rate of 10 kHz. This task had already been done as a part of a separate product development program, and hence, was no longer a task for this Phase I. By the time this program started, a standard short-pulse Lightwave product (Model 210-S) was already manufactured and available for pumping the OPO. Second, the proposal stated that the PPLN crystals would be purchased from Crystal Technology Inc. (CTI), Palo Alto, CA. Prior to the start of this Phase I, CTI denied our request to produce PPLN, so Lightwave developed the capability to fabricate PPLN in-house using Air Force SBIR Phase II funding. At the start of this program, Lightwave had already successfully produced small PPLN crystals for the Air Force. The PPLN crystals used in this program were produced at Lightwave using the electric-field poling technique described later in this report.

In the following section, we will present the experimental results of this program. The experimental results are organized by the two major program goals. In the first section the fabrication technique for the PPLN material will be described, along with the results of

our area and thickness scaling experiments. In the second subsection, we will describe the OPO results.

## 2.1 Fabrication of the PPLN Material

The full process for fabricating PPLN consists of five steps. These steps are: (1) buy bulk lithium niobate wafers; (2) send the wafers out for photo-lithography; (3) pole the wafers at Lightwave; (4) remove the photoresist and metal, and etch the wafers to reveal the pattern of the ferroelectric domains; (5) send out the etched wafers for polishing and coating of the apertures. All five of these steps must be correctly carried out to get a useful crystal, and although it sounds complicated, the yield of the process is quite high (~80% of our poling attempts yield device quality crystals). Below I'll describe each of these steps in greater detail and give an idea of the cost of each step.

(1) Buying the wafers is a straightforward step. We buy standard wafers used in the integrated optics business. The wafers are 3" in diameter, 0.5 - 1.0 mm thick, and have the orientation of the crystallographic axes indicated by flats cut into the sides of the wafer. The wafers are z-cut, and single crystal and are polished on both sides. Wafers cost ~\$200 a piece.

(2) The photolithography recipe we use was developed at Stanford University [5] and a schematic of a finished wafer is shown in Fig. 1. The recipe consists applying a 2  $\mu\text{m}$  thick layer of photoresist onto the +z wafer surface, and patterning the photoresist with UV irradiation through a suitable photomask. The mask contains the desired pattern which determines the QPM grating period and thus the OPO output wavelength. Lithography masks are standard products available from many vendors. After the exposure, the sample is immersed in developer which does the actual patterning of the photoresist. The pattern used to achieve optimal QPM in PPLN is a set of precisely spaced ridges of photoresist. The patterned wafer is then baked at 120 °C for 1 hour to "lock in" the pattern, and prevent its destruction by subsequent exposure to UV.

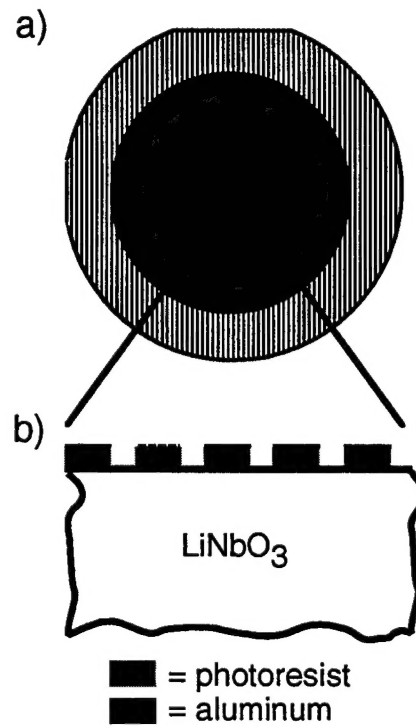


**Fig. 1** Schematic of photolithography used to fabricate PPLN. **a)** Shows the top view of an entire wafer. **b)** Shows a close up side view of the photoresist ridges. The spacing between adjacent ridges determines the output of the OPO and typically is 25 - 31  $\mu\text{m}$ .

Finally, a 200 nm layer of aluminum is evaporated through a shadow mask over the patterned photoresist. The shadow mask creates a round pattern of aluminum that is slightly smaller than the size of the o-ring used during the poling procedure. The grating periods needed for generating mid-IR wavelengths ( $\sim 30 \mu\text{m}$ ) , allow us to use photolithography that is considered to be "easy" by the electronics industry. The lithography step costs  $\sim \$250$  per wafer (plus a mask cost of  $\sim \$600$ ).

(3) The poling step is quite straight forward. The poling circuit is shown in Fig. 2. The threshold poling field is 21 kV/mm. We typically apply a field that is 3 - 4 kV/mm higher than this threshold. The series resistor controls the poling current ( $\sim 20 \mu\text{A}$ ) and other components are described in the figure caption. Our high voltage amplifier system can achieve 30 kV, which is sufficient for samples up to  $\sim 1$  mm in thickness. The input pulse to the amplifier controls the pulse amplitude and duration, and is produced by a digital function generator capable of making arbitrary waveforms. Typical poling pulse durations are 10 - 100 sec. The sample holder consists of two plexiglas blocks that sandwich the sample between two o-rings as shown in Fig. 3. Electrical contact to the sample surface is made via a liquid electrode ( $\text{LiCl}_2$ ). With the liquid electrode, the field is directly applied to the lithium niobate in the photoresist trenches (Fig. 1), and is electrically insulated from lithium niobate at the ridges. This difference in field strength between the ridges and the trenches is what produces the *periodic* poling. The liquid electrode is also important for controlling the fringe fields that can often lead to breakdown. The amount of time required to pole one wafer including set-up and clean-up is approximately 1 hour.

(4) Removal of the photoresist and metal is a standard lithography step, and is achieved by immersing the sample in sodium hydroxide, and then following this by immersion in acetone (to remove trace amounts of photoresist). To observe the pattern of the ferroelectric domains, the samples is immersed in HF acid. HF acid etches the  $+z$  and  $-z$  surfaces at a different rate, producing a step-like pattern on the wafer surface which is barely visible with the naked eye, but easily observed with an optical microscope.

(5) The dicing, polishing, and coating of the PPLN uses the standard techniques used for lithium niobate. The polished apertures are smaller than most polishing and coating

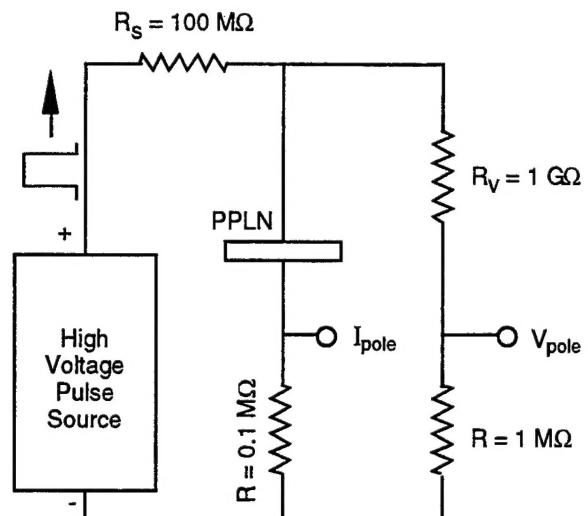
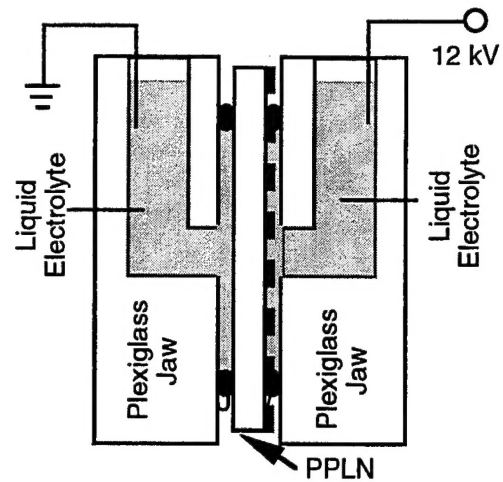


Fig. 2 Experimental poling circuit.  $R_s$  is a series resistor that controls the poling current.  $R_v$  is the voltage monitor.  $V_{pole}$  and  $I_{pole}$  are monitored by a digital oscilloscope.

vendors are used to, but this has not presented any major problem. The polishing and coating step dominates the cost per crystal. Typical costs are ~\$1000/crystal in small quantities or ~\$200/crystal in quantities over 20. Note that these costs are per *crystal* whereas the others are per *wafer*. Typically we can get >20 crystals per wafer, so prior to polishing and coating the per crystal cost is ~\$20\*1/50%yield = \$40. Hence total crystal cost is ~\$250 in large quantities. We give this estimate of crystal cost because it is critical to our decision to commercialize this technology. The low cost of this material relative to other crystals (e.g. ZnGeP<sub>2</sub> = \$30,000, AgGaSe<sub>2</sub> = \$7000, KTA = \$1500) makes it commercially very attractive.

At the start of this Phase I, state-of-the-art fabrication of PPLN produced crystals that were 0.5 mm thick, and had an area of ~20 mm x 20 mm. Using the fabrication procedure described above we have carried out a variety of crystal scaling experiments. For this Phase I program, we bought a total of seven wafers. Four were 0.5 mm thick, three were 0.75 mm thick, and two were 1 mm thick.

We first attempted to do the area scaling on the 0.5 mm thick wafers. We first made a new sample holder which could accommodate the larger lithium niobate crystals. We then bought larger masks and had the lithography pattern printed on entire wafers. The full wafers were loaded into the sample holder. We applied a number of pulses (4 or 5) each of which was ~12 kV in amplitude and 38 seconds long. At the end of the each pulse, we calculated the charge that had been transferred to the sample by integrating the current pulse ( $I_{pole}$  shown in Fig. 2). When the accumulated charge was ~2500  $\mu$ C, we knew that we had poled the entire area within the o-rings (a ~64 mm diameter circle) with an ~50% duty cycle. Of the four 0.5 mm thick wafers that we attempted to pole, we intentionally over poled one to see how the complete current and voltage traces look. The other three wafers were properly poled and yielded device quality domain patterns. We believe that poling full 3" wafers is no more difficult than poling smaller 20 mm x 20 mm pieces. We had no problems with breakdown, and in the future will only use full wafers in our poling procedure.



**Fig. 3** Poling sample holder. The PPLN is sandwiched between two o-rings held by plexiglas jaws. The jaws hold a liquid electrolyte which contacts the sample surface. The wire leads from the amplifier are dipped into liquid to complete the circuit.

To do the thickness scaling experiments, we diced one each of the 0.75 mm and 1.0 mm thick wafers into 1 cm x 1 cm pieces to give us plenty of trials to learn how to avoid breakdown due to the higher voltages associated with thicker crystals. We did not pattern these samples with photoresist, to reduce the cost of each trial. As expected, as the sample thickness increased, the likelihood of sample breakdown also increased. Through ~25 trials using unpatterned pieces, we learned that using thicker o-rings (0.125" thick vs. 0.063" thick), and carefully cleaning the plexiglas jaws between poling events significantly reduces the likelihood of breakdown. By the end of our experiments with unpatterned lithium niobate pieces, we could consistently pole them without breakdown.

Having gained confidence with the unpatterned samples, we then began to pole the patterned samples. We had three full 3" patterned wafers; two were 0.75 mm thick, and one was 1 mm thick. The first 0.75 mm sample broke down and cracked, but the second 0.75 mm thick sample and the 1 mm thick sample were poled successfully. The quality of the ferroelectric domain pattern of the two poled pieces was lower than what we have fabricated in the past, but we believe that this is mainly due to the particular photolithography run which produced the pattern (0.5 mm thick samples from this run also had a lower quality pattern) rather than due to the fact that these samples were thicker. We are now quite confident that with a few more tries that we will be able to fabricate 1 mm thick, device-quality PPLN pieces.

In summary, during this Phase I we improved our crystal fabrication process. By going to a larger fixture and using longer electrical pulses, we were able to scale the poled area from a ~17 mm diameter circle to a 65 mm diameter circle. We produced device quality 0.5 mm thick poled wafers with quasi-phasematched periods appropriate for mid-infrared generation. Scaling to larger areas increases the possible crystal length and significantly reduces the fabrication cost. We also demonstrated the feasibility of fabricating thicker crystals. We adjusted our fabrication recipe via trials on unpatterned lithium niobate crystals, and then successfully poled patterned 0.75 mm and 1.0 mm thick wafers. The domain pattern of these samples was not quite of device quality, but our work clearly demonstrates the feasibility of fabricating thicker crystals.

## 2.2 PPLN OPO Results

The second major area of research effort was in building and characterizing a high-power PPLN OPO. First, we will describe the pump laser, then we will describe the OPO.

### 2.2.1 The Pump Laser

The pump laser is a standard Lightwave Electronics Model 210-S. The experimental set-up is shown in Fig. 4, and consists of the laser, an isolator, an attenuator (half-wave-plate and thin film polarizer), a mode matching lens, and the OPO. Before pumping the OPO, we characterized the pump energy, pulse duration, and average power vs. repetition rate. The pulse energy was calculated from the average power which was measured after the isolator and attenuator, with the attenuator adjusted for maximum throughput. For CW and high repetition rates ( $>10$  kHz), the maximum average power after the isolator and attenuator was 4.8 W, if the attenuator and isolator were removed, the maximum output power was 5.4 W. Early in the experiments the OPO was pumped with the isolator and attenuator in the beam line. At the end of the experiments, the isolator and attenuator were removed to achieve the highest possible powers. Figures 5 and 6 show various quantities vs. repetition rate. Over 1.5 mJ/pulse was achieved for repetition rates of  $<1$  kHz, and pulse durations increased from 22 ns to  $\sim 150$  ns as the repetition rate was increased from 1 kHz to 50 kHz. The pulse duration at 10 kHz was  $\sim 40$  ns. The laser output was focused with a 150 mm focal length lens to produce a  $1/e^2$  radius of 90  $\mu\text{m}$ . The pump laser beam had some astigmatism (the focus in the horizontal and vertical planes was  $\sim 30$  mm apart). For the beam diameters used here, the astigmatism was not judged to be a limiting factor.

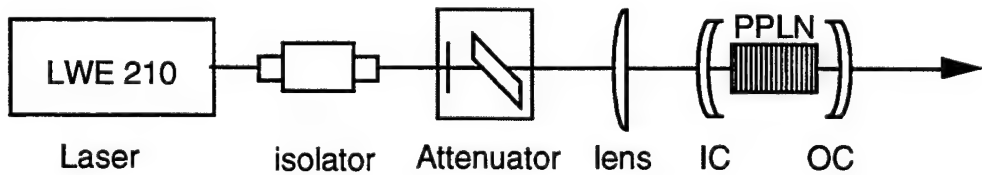


**Fig. 4** Schematic of the set-up for the Phase I OPO feasibility experiments. The attenuator consists of a half-wave plate and a thin film polarizer, IC = input coupler, OC = output coupler, and PPLN = periodically poled lithium niobate.

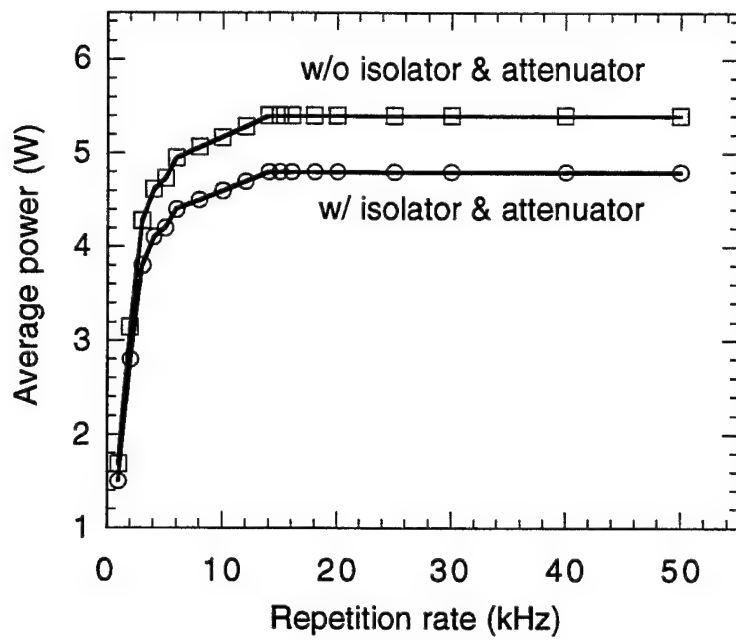


**Fig. 5** Average power of 1.064  $\mu\text{m}$  pump laser vs. repetition rate with and without the isolator/attenuator in the beam line.

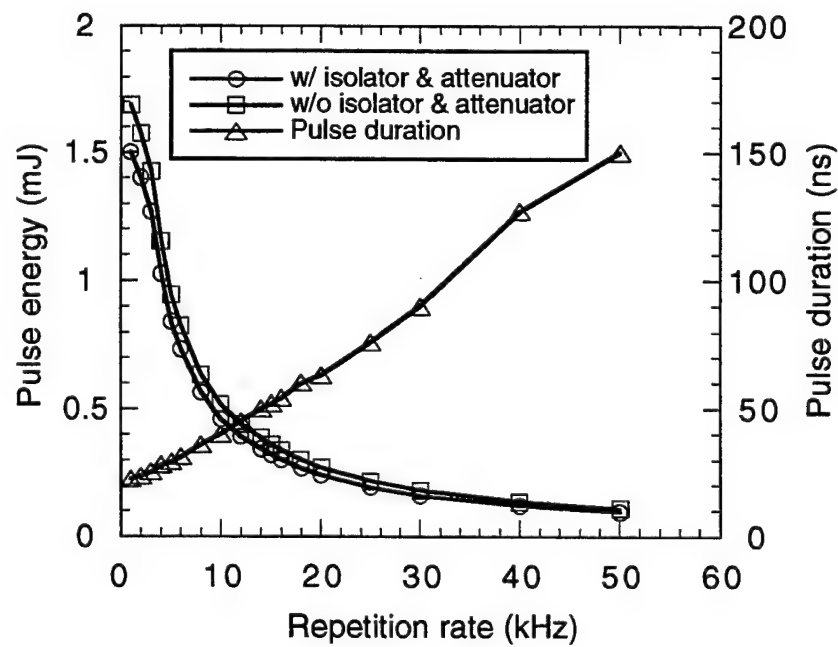


**Fig. 6** Pulse energy and duration vs. repetition rate. At 1 kHz pulse duration is 22 ns, at 10 kHz it is 40 ns, and at 30 kHz it is 90 ns.

### 2.2.2 The OPO Results

The OPO consisted of an input coupler, an output coupler, and a PPLN crystal. The baseline cavity had an input coupler with a 50 mm radius of curvature, and reflectivities of 3%, >99%, ~10% at the pump, signal, and idler wavelengths; and an output coupler that was flat with reflectivities of 2%, 60%, and 20% at the pump, signal and idler wavelengths. Several different PPLN crystals were used, all of which produced the same results (i.e. crystal-to-crystal variation is not measurable). The PPLN crystals were ~14 mm long, AR coated at the signal wavelength (losses at the idler wavelength were designed to be small, but were not directly measured). Crystals were used that had two different quasi-phasematching periods 29.5  $\mu\text{m}$  and 30  $\mu\text{m}$  which corresponded to the signal/idler wavelengths of 1.50  $\mu\text{m}$ /3.63  $\mu\text{m}$  and 1.54  $\mu\text{m}$ /3.45  $\mu\text{m}$ , respectively. The crystals were placed in an oven and operated at 70 °C. When operating PPLN at high repetition rates (>5 kHz) and at room temperature, we observed photorefractive (PR) damage which reduces the performance of the OPO. PR damage is easily observed by placing a white card behind the OPO and seeing the elongated green beam in the direction of the optic axis (the green is unphasematched SHG of the pump light). When the crystal is heated to 70 °C, the elongation begins to collapse at ~40 °C and is gradually reduced until at 60 °C it is no longer observable. This data is very consistent with bulk congruent lithium niobate. At 70 °C there is no observable photorefractive damage.

When the OPO is pumped above threshold, it begins to convert 1  $\mu\text{m}$  photons into 1.54  $\mu\text{m}$  and 3.5  $\mu\text{m}$  photons. A typical input vs. output curve is shown in Fig. 7. The oscillation threshold of ~1.4 W corresponds to an intensity of 26 MW/cm<sup>2</sup> and a fluence of 1.1 J/cm<sup>2</sup>. The average powers shown are "in-the-bucket" measurements, i.e. what the power meter reads (no losses are accounted for). To measure the data in Fig. 7, the pump had to be separated from the signal and idler. To measure the signal data, the beams were transmitted through a 1.064  $\mu\text{m}$  highly reflecting mirror (calcium fluoride substrate). The idler is removed by a filter on the front of the Melles-Griot power meter used to make the measurements. Leakage of the pump was checked for by turning off the OPO by detuning the OPO cavity. Less than 10 mW of light was measured with the OPO off. The transmission of the separation mirror at 1.54  $\mu\text{m}$  was measured to be 90% by placing a second, identical mirror in the path and noting the difference on the power meter. Hence, the actual amount of signal radiation produced is actually ~10 % higher than that shown in Fig. 7. To measure the idler data, the standard filter on the power meter was removed, and replaced by an uncoated piece of germanium. All three beams were then sent to the power meter, but the germanium only allows the 3.5  $\mu\text{m}$  light to pass. Again leakage was checked for by turning off the OPO. With the OPO off, the power meter read <10

mW Since the Ge filter was uncoated, it has a large Fresnel loss reflection. For Ge with an index of refraction of ~4, the uncoated transmission is ~50%. All idler data shown in Fig. 7 are the actual power meter reading multiplied by two. The transmission of the Ge filter was checked at 3.5  $\mu\text{m}$  by dispersing the OPO output with the tip of a glass prism and inserting the filter between the prism and the power meter. A power drop by a factor of two confirmed that the transmission of the Ge filter was what we had calculated it to be. In Fig. 7, the average power of the pump was varied via the attenuator, so that the pulse duration remains unchanged. Due to the excellent transmission of PPLN at all wavelengths, we did not expect to see any thermal effects. The linear output vs. input indicates that no thermal effects were present, and a qualitative check of the signal beam with an IR card showed a nice round beam that can be highly collimated.

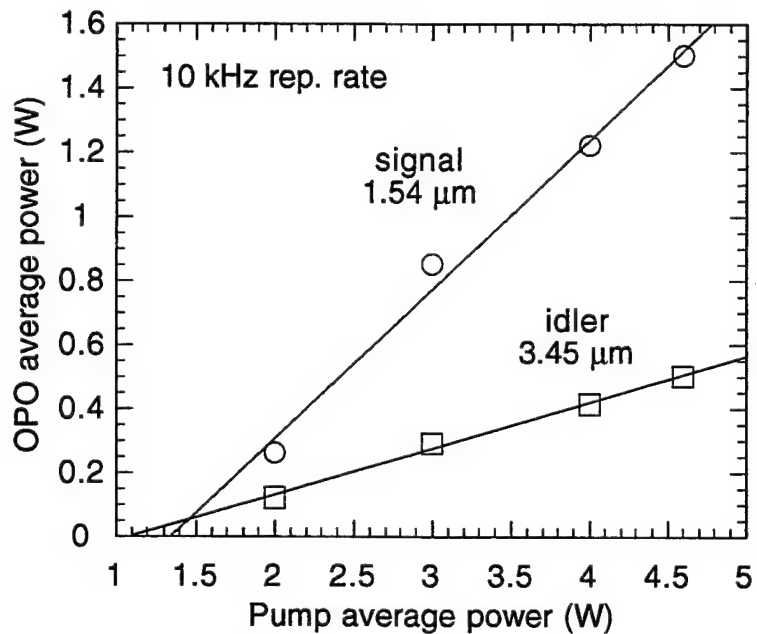


**Fig. 7** Input vs. output for PPLN OPO operating at 10 kHz with the attenuator and isolator in the pump beam (limiting the pump power to <5 W).

In past lithium niobate OPOs, optical damage (not photorefractive damage) has been an issue [6] and we were concerned about how PPLN would fare as the average powers were increased. Fortunately, damage was not an issue in collecting the data presented here. At no time during this work was any crystal or optic damaged other than on two occasions when we deliberately damaged a crystal to learn what the actual damage threshold was. The damage was induced by running the OPO at 10 kHz with the attenuator set for maximum throughput and gradually reducing the repetition rate (thereby increasing the peak

power, see Fig. 6) until the crystal damaged. On both trials the crystal damaged at 3-4 kHz, meaning that the damage threshold is  $380 \text{ MW/cm}^2$  or  $10.2 \text{ J/cm}^2$ . I should point out that this is a "laser-conditioned" damage threshold (lithium niobate is known to have a higher damage threshold after it has been irradiated by a laser beam). The damage threshold is a factor of  $\sim 15$  higher than the oscillation threshold, a very nice margin to work within. Saturation of the OPO conversion efficiency was observed to occur at 4 times the oscillation threshold, so operating the OPO at higher intensities has no advantages. The low operating intensity of PPLN ( $\sim 100 - 150 \text{ MW/cm}^2$ ) reduces the likelihood of damage of the OPO cavity mirrors. Crystals such as KTA may have very high damage thresholds, but this only transfers the damage problem from the OPO crystal to the OPO mirrors. The very high nonlinear coefficient of PPLN, allows low operating intensities, making it much easier to build sufficiently damage resistant OPO mirrors.

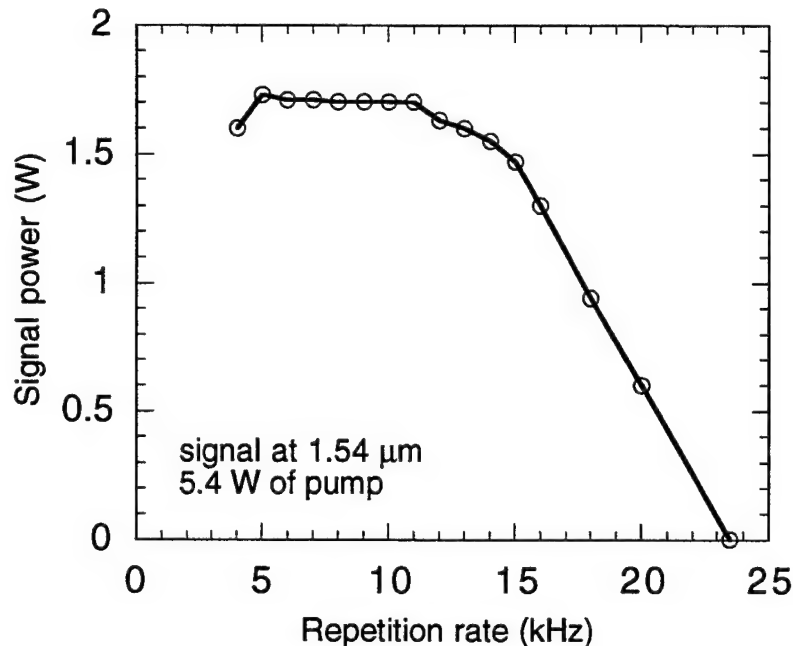


**Fig. 8** Signal output vs. repetition rate (the idler follows a similar curve with the peak at  $\sim 0.55 \text{ W}$ ). The performance is virtually flat over 5 - 15 kHz. The output on the low rep. rate side is limited by damage, and on the high rep. rate side by lack of peak power. If rep. rates outside of the 5 - 15 kHz range are desired, one simply needs to adjust the spot size of the pump to optimize the performance at the desired rep. rate (see Fig. 9).

To get the very most average power out of the system, we removed the attenuator and isolator. The output power of the laser could be controlled by varying the diode current, but the simultaneous change in the beam properties and pulse duration would give nebulous results. Instead the repetition rate was varied while the pump power was fixed.

Fig. 8 shows how the output power varies with repetition rate. The performance is nearly flat over 5 - 15 kHz due to the saturation of the OPO conversion efficiency as the pumping is increased. On the high repetition rate side, the peak power is continually reduced until the OPO reaches threshold at ~24 kHz. However if higher repetition rates are desired, one merely needs to focus the pump beam a bit tighter to increase the peak intensity. The noncritical quasi-phasematching afforded by PPLN allows optimal focusing that could be 10 times more intense than that used in the work described here.

To test this idea, we attempted to run the OPO at higher repetition rates by focusing the pump beam tighter. We replaced the 150 mm focal length lens with a 100 mm lens, and moved the OPO new position of the focus. We also replaced the R=60% output coupler with a high reflector to minimize the threshold. With these simple changes, we retook data similar to that shown in Fig. 8, but at higher repetition rates. This is shown in Fig. 9.

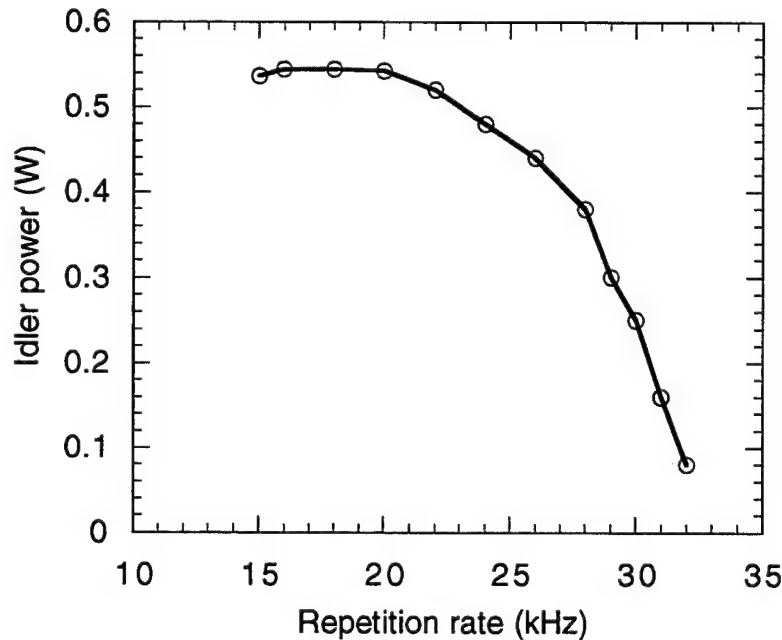


**Fig. 9** Idler power vs. repetition rate over the range of 15 - 32 kHz. This higher repetition rate is attained by focusing the pump beam tighter and using a high reflector (at the signal wavelength) as an output coupler.

Note that instead of being optimized at ~10 kHz, the conversion is now optimized for 15 - 20 kHz, with reasonable conversion all the way out to 30 kHz. PPLN's ability to noncritically phasematch any wavelength in its transparency range is a key advantage for trying to attain operation at very high repetition rates (such as 50 kHz or even CW) with a modest pump source of ~5 W. Other crystals such as KTP or KTA have a difficult time

operating in this very high repetition rate regime (>20 kHz) where peak powers are low (unless the pump lasers are very large (>50 W)).

Although the technical objectives of this program did not include this, we were able to measure OPO output vs. wavelength over the range of 2.7 - 4.8  $\mu\text{m}$ . This data gives a indication of how useful PPLN might be for generating radiation in the Band IV atmospheric window. We used a piece of PPLN that is 19 mm long, uncoated, and has a series of QPM gratings on it (26  $\mu\text{m}$  - 31  $\mu\text{m}$  in 1  $\mu\text{m}$  steps). This piece was fabricated by Larry Myers of Stanford University [7]. We plan on fabricating similar pieces in the future. Fig. 10 shows the data. We should strongly point out that at 3.5  $\mu\text{m}$  the output power is 300 mW instead of the 0.5 W that we more typically saw with the single grating pieces. This difference is primarily due to the uncoated surfaces (14% per surface, causing more than a 50% round-trip loss for the signal). Fig. 10 shows significant output in the 4.5  $\mu\text{m}$  region. Transmission data of LiNbO<sub>3</sub> taken in the 3 - 6  $\mu\text{m}$  range indicates

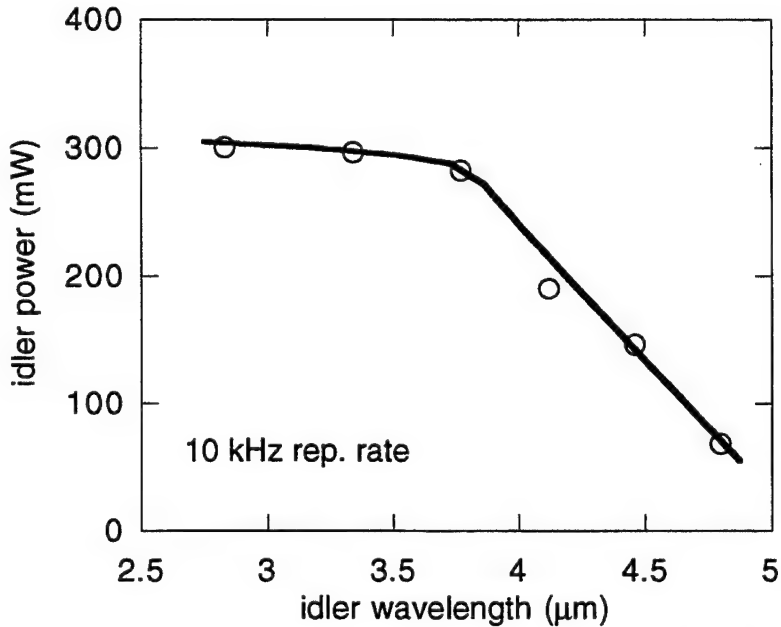


**Fig. 10** Output of multi-grating PPLN OPO vs. wavelength at 10 KHz repetition rate, with 4.7 W of pump. This piece of PPLN had no AR coatings, and hence was very lossy. To estimate how much output could be obtained in a more optimized OPO (with AR coatings and a similar amount of pump light), multiply the ordinate value by a factor of ~2.

that the loss for e-polarized light is significantly less than for o-polarized light [7]. This is fortuitous for PPLN OPOs, since all three waves are e-waves (for birefringently phasematched lithium niobate OPOs the idler must be an o-wave). A comparison with KTA, indicates that PPLN was about the same loss per unit length as KTA at 4.5  $\mu\text{m}$ .

Since PPLN has much higher gain per unit length than KTA (allowing the use of shorter crystals), one concludes that PPLN may be a better candidate for high power radiation at  $4.5\text{ }\mu\text{m}$ . This data is preliminary, future work should be aimed at making an optimized PPLN OPO that generates  $4.5\text{ }\mu\text{m}$  light.

Throughout all of our experiments we monitored the pump depletion. The temporal trace of the depleted pump along with the undepleted pump is shown in Fig. 11a. For all configurations that we investigated, the depleted pump pulse had a unusual second peak (shown with a white arrow in Fig. 11a. The small first peak, is typical and is due to the rise time of the OPO. The second peak is mysterious, and closely follows the shape of the undepleted pump pulse, maintaining a constant instantaneous pump depletion of  $\sim 55\%$ . The second peak was observed at all repetition rates and pulse durations. We know that this secondary hump is not intrinsic to PPLN OPOs. Fig. 11b shows a similar pump depletion trace of a PPLN OPO, pumped by a different pump laser with shorter pulse durations (note the different time scales for Figs. 11a and 11b). The pump depletion trace of Fig. 11b is typical for OPOs, and exhibits instantaneous depletions of  $\sim 75\%$ . At present, we do not understand the cause of the second peak in Fig. 11a, but hope to explore this in Phase II. Eliminating the second peak would increase conversion efficiency and output powers by a factor of  $\sim 1.3 - 1.5$ , hence, there is a lot of motivation to understand this phenomenon.

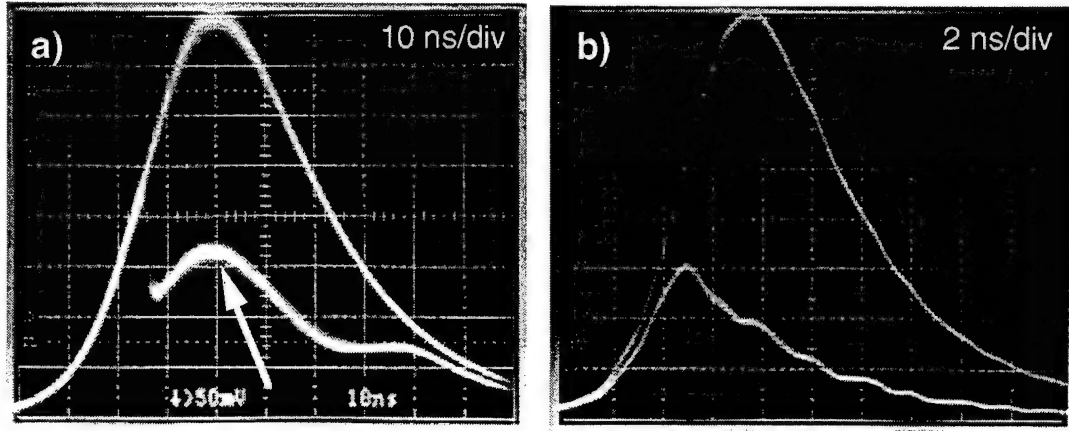
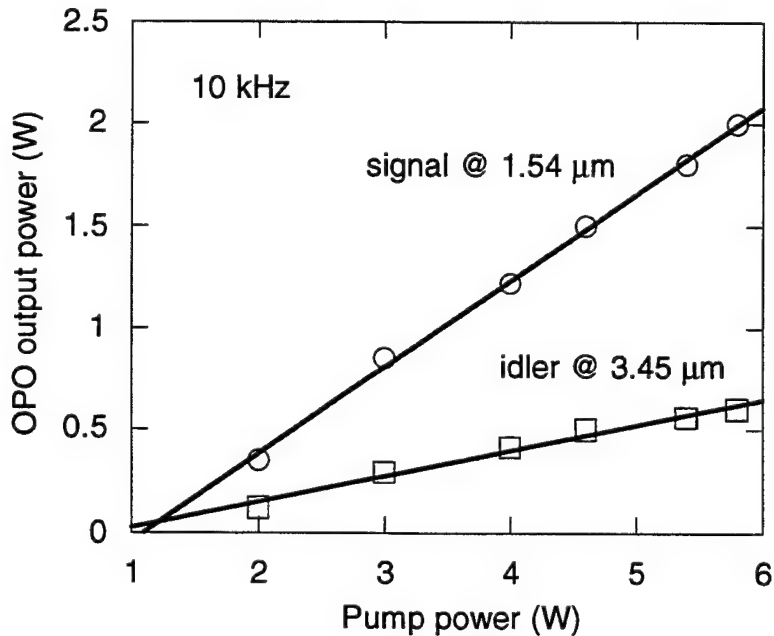


Fig. 11 Temporal profile of the depleted pump pulse measured in Phase I (a), and a more typical looking depleted pump pulse measured with a different pump laser (b). In both figures the top trace is the undepleted pump (OPO off), and the bottom trace is the depleted pump (OPO on). The second peak in the lower trace of (a), identified by the white arrow, clamps the instantaneous conversion efficiency of the device to 55%, whereas the pump depletion in (b) is over 70 %. In Phase II, we hope to understand the origin of this peak and eliminate it.

At the end of our experiments we fully optimized the pump laser to get the highest pump levels (the thermal load was tweaked a bit). With 5.8 W of pump, 2.0 W of signal light and 0.6 W of 3.5  $\mu\text{m}$  idler light was reproducibly available. The values obtained with 5.4 W and 5.8 W of pump are included with the data of Fig. 7, and shown in Fig. 12. Note that the signal and idler vs. pump are linear up to the ~6 W pump level indicating no thermal effects. In the proposal, we had a goal of 1 W of 3.5  $\mu\text{m}$  light (from 6 W of pump) which requires a 55% pump photon conversion efficiency [8]. Although 0.6 W is less than the 1 W goal, we did achieve the conversion efficiency goal. With 5.8 W of pump, we measured 2 W of 1.54  $\mu\text{m}$  light, which means we really are making 2.2 W (the pump separator has a loss of 10 %) which yields a pump photon conversion efficiency of 58%. If the Manely-Rowe condition were obeyed in our output (i.e. the cavity losses for the two wavelengths were equal) this would result in 0.97 W of idler light. We attribute the lower idler output to the 20% loss of the idler at the output coupler, and to (unmeasured) losses at the crystal surfaces. It has been our experience that coating vendors need a couple of tries to get high performance coatings, and in a Phase I program, we only got one try. Thus by fully optimizing the coatings, etc., and using a full 6 W of pump light, we would have obtained our goal of ~1 W of 3.5  $\mu\text{m}$  radiation.



**Fig. 12** Input vs. output of PPLN OPO with up to 5.8 W pump. the four lowest data points were taken with the isolator and attenuator in the pump beam. The fifth data point (5.4 W pump power) was taken with the isolator and attenuator removed. The sixth data point (5.8 W) was taken with the isolator and attenuator removed after the pump laser was "tweaked". The linear output vs. input indicates minimal thermal distortion in the crystal.

### **2.3 Phase I Conclusions**

We believe that these results show that PPLN can be used as a high power mid-IR OPO material. We have demonstrated high power (Watts) operation at repetition rates of 1 - 30 kHz, and generated wavelengths over the range of 1.35 - 1.66  $\mu\text{m}$  (signal) and 2.7 - 4.8  $\mu\text{m}$  (idler). PPLN has many intrinsic advantages over other crystals. Future optimization such changing crystal length, resonating the idler, and really working hard to eliminate the coating losses will bring even better results and higher average powers.

## **3.0 Potential Commercial Applications**

A compact, efficient, and inexpensive source in the mid-infrared spectral range is commercially attractive for a large number of laser radar, spectroscopic and remote sensing applications. Presently, tunable, fieldable mid-infrared sources are not available, which has hampered applications, two of which are described in further detail below.

### **3.1 Eye-safe laser radar and range finders**

A coincidence of good atmospheric transmission, maximum eye-safety, and high detector sensitivity has prompted interest in the 1.54  $\mu\text{m}$  spectral region for laser radar and range finder applications. While one can obtain 1.54  $\mu\text{m}$  radiation from an Erbium solid-state system, the low gain, and/or poor thermal properties of this system has precluded their use. Also frequency shifting of 1  $\mu\text{m}$  radiation via Raman shifting in methane has been demonstrated, but issues of efficiency, complexity, and beam quality again have precluded the use of this technique. An all solid-state approach of 1  $\mu\text{m}$  lasers pumping KTP OPOs has seemed most promising. These customers are contracted by the Federal Government to build mid-infrared imaging systems. These customers believe that their system, with a suitable mid-infrared laser source, would initially sell in quantities of 50 - 100 per year. The output power and repetition rates we demonstrated in Phase I meet the customer needs, but the pulse durations are a factor of 2 - 3 too long. In the Phase II program, one the goals would be to reduce the pulse duration. If we can demonstrate the required pulse duration, pulse energy, and repetition rate, these customers have agreed to pay the non-recurring engineering costs needed to engineer the transmitter system. The main obstacle to using our technology in this application is the long pump pulse duration, which we would directly address in the Phase II program.

### 3.2 Hydrocarbon Detectors

In the spectral range of 3.1 - 3.6  $\mu\text{m}$  most light hydrocarbons such as methane, ethane, propane, etc. exhibit strong absorption features. Various large and costly differential absorption lidar systems (DIAL) have been built to remotely measure concentrations of these important molecules. Remote detection of light hydrocarbons in the 3  $\mu\text{m}$  region is important for applications such as: (1) oil exploration; (2) natural gas line leak detection; (3) greenhouse gas monitoring; (4) drug enforcement; and (5) methane detection in coal mines. In all of these applications, the goal is to measure the presence, and in some cases the concentration of a specific molecular species. LIGHTWAVE Electronics has been contacted by the developer of the commercial GasVue™ system. This system uses a laser to visualize gas clouds and works as follows. A CW CO<sub>2</sub> laser is scanned over a target, and the scattered light is viewed with an infrared camera. The wavelength of the laser is chosen to be strongly absorbed by the gas of interest, and hence a cloud shows up on the camera screen as a dark area. The use of a CW CO<sub>2</sub> laser makes the image update rate very slow (one image takes a few seconds) because the laser must be rastered in two dimensions. The limited and noncontinuous tuning range of the CO<sub>2</sub> laser also limits the number of gases that can be viewed. The gas of greatest commercial interest is methane, which has a strong absorption at  $\sim 3.3 \mu\text{m}$ . With a pulsed laser source, the entire image could be captured in a few pulses, allowing a much faster update rate. Pulsed PPLN OPOs could address this application quite nicely, if the linewidth of the device could be narrowed to fit within the spectral features of methane. The application requires a linewidth of  $< 2 \text{ cm}^{-1}$ . The natural linewidth of a PPLN OPO at 3.3  $\mu\text{m}$  is  $\sim 10 \text{ cm}^{-1}$ . The potential customer is waiting to see whether we can control the linewidth of our OPO to meet the specification before proceeding any further. We hope to demonstrate the feasibility of narrowing the linewidth of our OPO with an intracavity acousto-optic tunable filter (AOTF). Although the AOTF does not have the best wavelength resolution, it does allow tuning with no moving parts, creating a very rugged system. Once an OPO can be demonstrated to meet the requirements of the developer, we can continue to move towards engineering devices to meet the needs of this application.

The GasVue system is only one example of the power of spectroscopy for remote detection. The lack of line narrowed sources, both pulsed and CW, in the mid-infrared, is the major obstacle to realization of many detection applications.

## **4.0 Recommendations for Phase II**

This Phase I program demonstrated a multi-watt PPLN OPO for the first time. The input vs. output for signal and idler wavelengths of  $1.54\text{ }\mu\text{m}$  and  $3.5\text{ }\mu\text{m}$  are linear to pump levels of  $\sim 6\text{ W}$  (the maximum pump level available from our pump laser). The ultimate average power scaling limit for PPLN has not yet been reached. PPLN is still a relatively new material, and the main goal of a Phase II program would be to continue to explore the average power limit for PPLN OPOs particularly in the important  $4.5\text{ }\mu\text{m}$  atmospheric window. The four major topics that will be proposed for Phase II are given below.

### **4.1 Pump laser development**

- To make higher power mid-infrared radiation, we need a higher power pump laser ( $\sim 15\text{ W}$ ). We don't plan a major development effort here, but will extend the basic design of our commercial laser product (Model 210-S) by adding extra gain module(s) to the cavity.
- We will also work towards obtaining shorter pulses (this is important for the  $1.5\text{ }\mu\text{m}$  LADAR applications). To get the pulses to be as short as required (<15 ns), we will try a higher gain material such as Nd:YVO<sub>4</sub>.

### **4.2 PPLN Material Development**

- We will follow up the feasibility study in Phase I by fabricating device quality 1 mm thick crystals (present crystals are 0.5 mm thick).
- Multiple/tunable gratings on a single PPLN chip for tunability. Stanford University has already demonstrated this, but Lightwave Electronics has not. The multiple/tunable gratings allow broad tuning with a single crystal.
- Monolithic OPOs (for improved device ruggedness). The main issue here is how accurately the two polished surfaces can be aligned for the thin crystals.
- Elimination of photorefractive damage at room temperature. MgO:PPLN, and chirped quasi-phasematching gratings are two approaches to be explored.

### **4.3 PPLN OPO Device Development**

- Optimize the  $4.5\text{ }\mu\text{m}$  output power (optimize crystal length, cavity configuration, and evaluate performance at Watt level average powers).

- Evaluate the operation of the PPLN OPO in a CW mode. Ideally an infrared countermeasures (IRCM) source would be CW, and PPLN is the best CW mid-IR OPO material. Calculations indicate that CW thresholds (singly resonant) should be <5 W. The pump laser of section of 4.1 can be run in a CW mode, and by focusing the pump light tighter, and reducing the losses in the OPO cavity, CW (singly resonant) operation could be demonstrated and characterized. Of particular interest is the devices amplitude stability, and how well the OPO output can be modulated by modulating the pump.
- Narrow the linewidth of the PPLN OPO. Although IRCM applications don't require it, many commercial applications such as environmental and industrial monitoring, require linewidths narrower than the "natural" linewidth of the OPO. The broad linewidth of OPOs is a major stumbling block that prevents their use in a broader range of markets. We would like to try inserting an acousto-optic tunable filter (AOTF) in the OPO cavity. AOTFs have high efficiency, moderate resolution, and contain no moving parts.
- Test the breadboard of the deliverable. This involves doing the detailed characterization prior to assembly of the deliverable. We will try to understand and eliminate the second pump depletion peak shown in Fig. 11a. Goals for the breadboard are to demonstrate separate OPOs with outputs of >3 W at 2.1  $\mu\text{m}$ , >2 W at 3.5  $\mu\text{m}$ , and >1 W at 4.5  $\mu\text{m}$ .

#### **4.4 Package the deliverable**

The exact configuration of the final deliverable depends on the preceding breadboard characterization. A baseline configuration is shown in Fig. 13. We will fully package the pump laser described in section 4.1. All LIGHTWAVE Electronics commercial products have rugged, hermetically sealed packages that are well known in the laser industry. The pump laser will be assembled using the patented technology developed for our 200 series products. This laser will be put in the sealed, commercial package (laser head: 5.5" x 3.4" x18.5", 9 kg; power supply: 19" rack mount x 3.5", 5 kg; chiller: 19" rack mount x 10.5", 40 kg). The laser controls such as repetition rate, diode current, etc. are all accessed on the power supply. No controls are at the laser head or chiller. This pump laser will be mounted on a suitable base, that holds a "fixed" OPO and a "tunable" OPO.

The baseline fixed OPO will be monolithic although an external cavity OPO could be substituted. The fixed OPO will be fastened to the base with the patented techniques used in our commercial products (gluing and soldering). The "fixed" OPO will operate at  $\sim 4.5 \mu\text{m}$ , and will be narrowly tunable with temperature if the crystal is placed in an oven. The other OPO is a "tunable" OPO. The tunable OPO is a completely separate structure, mounted on its own base. The aligned cavity mirrors are fixed to the base (no adjustments), and the multiple/fanned crystal is mounted on a translation stage. Turning the micrometer screw, translates the crystal which tunes the device. The tuning range is chosen to cover any of the three atmospheric transmission windows. The tunable OPO is pumped by diverting the pump beam with a kinematically mounted mirror. The configuration shown in Fig. 13 is the baseline configuration, and can be changed if necessary. Not shown in Fig. 13 are crystal ovens, beam separation optics (to separate the mid-infrared from the near infrared), and enclosures for the OPOs.

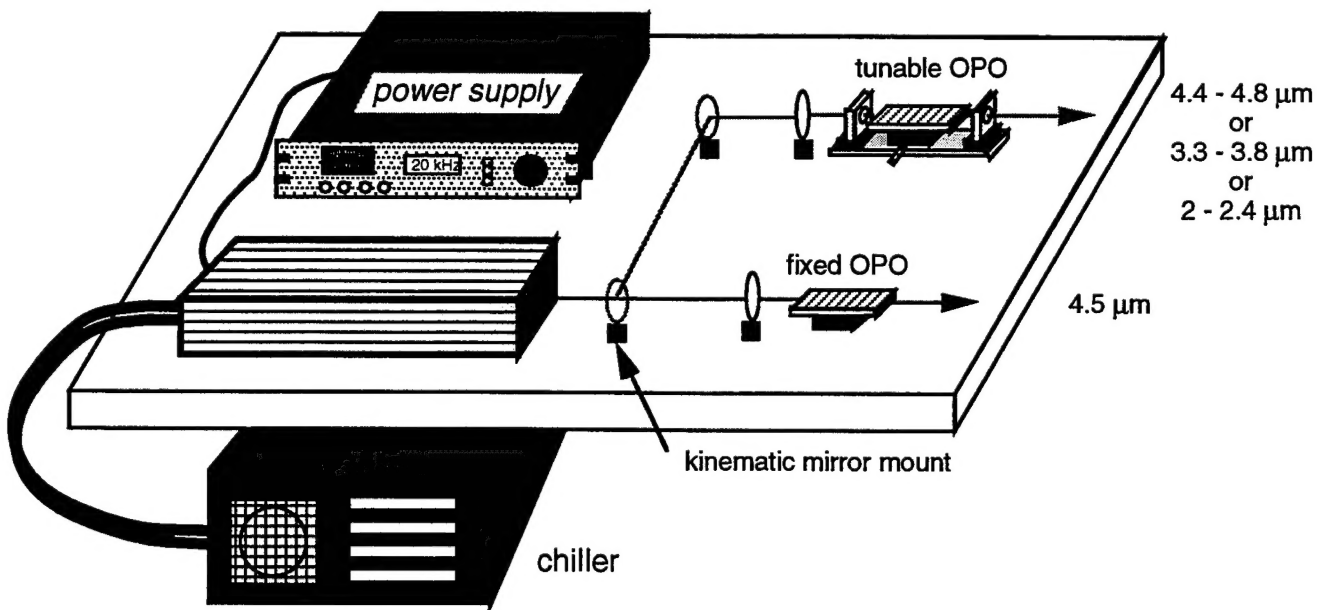


**Fig. 13** A simplified schematic of the deliverable. Shown are the hermetically sealed laser head, its power supply, and chiller. There are two OPOs. The fixed OPO is a monolithic design which emits  $4.5 \mu\text{m}$  radiation. The tunable OPO is an external cavity OPO with a fanned or multiple grating. By turning the micrometer screw and translating the crystal, the OPO output can be tuned over the atmospheric transmission windows. The external cavity of tunable OPO will be mounted on its own base, and the mirrors will be fixed for better device stability. A kinematic mirror mount selects which OPO is to be operated. Not shown are crystal ovens (for tuning of the fixed OPO, beam separation optics (to separate the mid-infrared from the near infrared), and enclosures for the OPOs.

## 5.0 Conclusions

This Phase I program resulted in the first demonstration of a multi-watt output from a PPLN OPO. PPLN is a promising new mid-infrared nonlinear optical material with significant advantages over existing materials. The Phase I program showed that the 6 W average power pump level is clearly below the limit for this material. Future work will be directed at determining the scaling limit for PPLN, and improving the material fabrication process.

## 6.0 References

- [1] J. A. Armstrong, N. Bloembergen, J. Ducing, and P. S. Pershan, "Interactions between light waves in a nonlinear dielectric", *Phys. Rev.* **127**, 1918 (1962).
- [2] M. M. Fejer, G. A. Magel, D. H. Jundt, and R. L. Byer, "Quasi-phasematched second harmonic generation: tuning and tolerances", *IEEE J. Quant. Electron.* **28**, 2631 (1992).
- [3] D. E. Withers, G. Robertson, A. J. Henderson, Y. Tang, Y. Cui, W. Sibbett, B. D. Sinclair, and M. H. Dunn, "Comparison of lithium triborate and barium borate as nonlinear media for optical parametric oscillators", *J. Opt. Soc. Am. B* **10**, 1737 (1993).
- [4] G. D. Boyd, and D. A. Kleinman, "Parametric interaction of focused gaussian light beams", *J. Appl. Phys.* **39**, 3597 (1968).
- [5] L. E. Myers, R. C. Eckardt, M. M. Fejer, R. L. Byer, W. R. Bosenberg, and J. W. Pierce, "Quasi-phasematched optical parametric oscillators in bulk periodically poled lithium niobate", accepted for publication *J. Opt. Soc. Am. B*, November 1995.
- [6] S. J. Brosnan and R. L. Byer, "Optical parametric oscillator threshold and linewidth studies", *IEEE J. Quant. Electron.* **QE-15**, 415, (1979).
- [7] L. E. Myers, R. C. Eckardt, M. M. Fejer, R. L. Byer, and W. R. Bosenberg "Grating tuned, quasi-phasematched optical parametric oscillator in periodically poled LiNbO<sub>3</sub>", submitted for publication *Opt. Lett.*
- [8] We define the pump photon conversion efficiency as the sum of the signal and idler powers measured divided by the pump power delivered to the OPO.